

JFSP Project Final Report

Project Title: Burn Severity Mapping Using Simulation Modeling and Satellite Imagery

Date: April 2008

JFSP Project Number: 05-1-1-12

Principal Investigators: Robert E. Keane and Eva C. Karau

Federal Cooperator: Elizabeth Reinhardt

Intended Outlet: International Journal of Wildland Fire

Table of Contents

JFSP Project Final Report.....	1
Table of Contents.....	1
Abstract.....	2
Introduction.....	3
Background.....	6
Image-based Burn Severity Mapping	6
Fire Effects Simulation Modeling.....	9
Synergy of burn severity mapping approaches.....	11
Project Objectives	12
Methods.....	12
Study Areas.....	13
Field Sampling.....	15
Satellite Imagery	17
FIREHARM Simulations.....	19
Plot-based Simulations.....	19
LANDFIRE-based Simulations	21
Comparison and Validation	22
Results.....	22
Field Sampling.....	22
FIREHARM and Δ NBR Validation	23
Burn severity mapping.....	24
Discussion.....	25
Acknowledgements.....	31
References.....	31
Tables.....	40
Figures.....	46

Abstract

As wildfires become an increasingly important issue affecting our nation's landscapes, fire managers must quickly assess possible adverse fire effects to efficiently allocate resources for rehabilitation or remediation. While burn severity maps derived from satellite imagery can provide a landscape view of relative fire impacts, fire effects simulation models can also provide spatial fire severity estimates along with the biotic context in which to interpret severity. In this project, we evaluated two methods of mapping burn severity for four wildfires in western Montana using 64 plots as field reference: 1) an image-based burn severity mapping approach using the Differenced Normalized Burn Ratio (Δ NBR), and 2) a fire effects simulation approach using the FIREHARM model. We compared the ability of these two approaches to estimate field-measured fire effects and found that the image-based approach was moderately correlated to percent tree mortality ($r = 0.53$) but had no relationship with percent fuel consumption ($r = -0.04$). The FIREHARM model was moderately correlated with percent fuel consumption (0.33) and weakly correlated with percent tree mortality ($r = 0.18$). Burn severity maps produced by the two approaches were quite variable with map agreement ranging from 33.5% and 64.8% for the four sampled wildfires. Both approaches had the same overall map accuracies when compared to a sampled composite burn index (57.8%). Though there are limitations to both approaches, we believe these techniques could be used synergistically to improve burn severity mapping capabilities of land managers, enabling them to meet rehabilitation objectives quickly and effectively.

Introduction

Each year, thousands of acres of wildlands are severely burned in wildfires due to high canopy and surface fuel loadings that have accumulated over seven decades of fire exclusion (Ferry *et al.* 1995; Keane *et al.* 2002). Most land management agencies in the United States work in accordance with the National Fire Plan and agency guidelines to assess the effects of fire and mitigate damage through rehabilitation activities such as reforestation, erosion control, invasive weed treatment, and habitat restoration (NWCG 2003). This requires accurate, efficient and economical methods to assess the severity of a fire at a landscape scale (Brennan and Hardwick 1999). Burn severity mapping technology is a critical tool in the process of identifying severely burned areas and facilitating prudent implementation of costly rehabilitation and restoration efforts (Eidenshink *et al.* 2007; Lachowski *et al.* 1997; Miller and Yool 2002).

Burn severity maps are useful to scientists and managers for a variety of applications. Spatial maps of fire effects are useful for delineating fire regimes (Morgan *et al.* 2001), linking landscape patterns and scales of disturbance processes (Chuvieco 1999; Turner *et al.* 1994; White *et al.* 1996), assessing potential for post-fire vegetation recovery or reestablishment (Diaz Delgado *et al.* 2003; Jakubauskas *et al.* 1990; Lentile *et al.* 2007; Lopez Garcia *et al.* 1991; Turner *et al.* 1999; White *et al.* 1996), evaluating wildlife habitat disturbance (Zariello *et al.* 1996), and gauging the effects of fire on species of concern (Kotliar, 2003). Burn severity maps can also be used to evaluate if the fire had beneficial consequences to the burned landscape (i.e., an unplanned ecosystem

restoration treatment) by comparing historical burn severity distributions to severities contained in the recently burned area (Pratt *et al.* 2006). In the United States, burn severity maps are developed operationally from two main sources. Currently, the multi-agency Monitoring Trends in Burn Severity Project systematically creates and archives burn severity maps in a national fire atlas to allow scientists and managers to assess trends in fire characteristics (Eidenshink, *et al.* 2007). The Burned Area Emergency Rehabilitation (BAER) is a US Forest Service and Department of Interior program initiated to provide burn severity maps as rapid response tools for post-fire rehabilitation efforts (Lachowski *et al.* 1997; USFS 1995).

There is often confusion among scientists and managers involving the terminology used to describe the impacts or effects of fire across a wide variety of ecosystem components (Lentile *et al.* 2006). In this paper, the term *fire severity* denotes the magnitude of fire-caused damage to vegetation. Discrete, ordinal indices of fire severity are often used to summarize the complex and interacting effects of a fire (Ryan and Noste 1985). The advantage of these indices is that they integrate a variety of information and summarize it into succinct, intuitive categories. The disadvantage is that they are overly simplistic and rarely address all possible management concerns that require an estimate of severity. For example, a fire severity estimate that emphasizes soil erosion potential would use a different classification of severity as compared to a severity estimate of fire-caused tree mortality or the amount of surface fuel consumed. In this paper, we follow the terminology convention initiated by Reinhardt *et al.* (2001), where *first order fire effects* are the direct results of the combustion process (plant injury or mortality, fuel

consumption, soil heating and smoke production) and *second order fire effects* are the indirect effects of fire and other processes that occur over a longer time frame (erosion, smoke dispersion, vegetation succession). These are the unambiguous, biophysically dimensioned measures of the effects of fire that vary on a continuous scale. As this project was primarily focused on the immediate effects of fire, we use the more general term *fire effects* in reference to first order fire effects. We use the term *burn severity* somewhat interchangeably with the descriptive term fire severity, but more specifically to describe the magnitude of combined fire effects using an ordinal index value, whether it is derived from a satellite imager, a fire effects model, or field sampled data.

We considered two major approaches to the creation of useful burn severity maps: remotely sensed imagery and simulation modeling. Remotely sensed imagery from space and airborne platforms has been used to map burn severity at landscape and regional scales for over two decades (White *et al.* 1996; Zariello *et al.* 1996; Kushla and Ripple 1998; Bigler *et al.* 2005; Cocke *et al.* 2005; Duffy *et al.* 2007; Eidenshink *et al.* 2007; Hammill and Bradstock 2006; Hudak *et al.* 2007; Lentile *et al.* 2007) and this technology is clearly useful for spatial post-fire resource management (Brennan and Hardwick 1999; Greer 1994; Sunar and Ozkan 2001). Simulation modeling is another somewhat newer tool that can provide spatial estimates of fire effects provided high quality input spatial data layers are available. FIREHARM, a landscape scale fire effects research model, is designed to output physically based estimates of fire effects that are then used to describe burn severity quantitatively (Keane *et al.* [in prep]). Both approaches have limitations

associated with implementation, data availability, required expertise, and potential accuracy (Keane *et al.* [in prep]).

In this study, we evaluated and compared satellite and model-derived approaches to map burn severity and fire effects, and then assessed the potential for combining these two approaches into a suite of fire management tools. A blending of both approaches might help fire management meet the need for the most accurate and rapid assessment of spatial fire severity given time, funding, and resource constraints. It is important that the fire manager understand the benefits and limitations of both approaches so that burn severity maps can be interpreted in the context of the proposed management activity and development approach.

Background

Image-based Burn Severity Mapping

Remote sensing technology makes it possible to gather information about a target from a location that is remote from the target itself, facilitating a unique perspective for the observation of earth features. A sensor on an airborne or satellite platform can detect energy emanating from the earth's surface and different features tend to exhibit distinctive reflectance characteristics throughout the electromagnetic spectrum (Campbell 1996). For example, healthy vegetation typically absorbs or reflects more energy in certain wavelengths compared to non-vegetated surfaces, allowing differentiation of these

features on satellite imagery (Verbyla 1995). This principle, along with the repeatability of measurements, allows satellite image technology to have great utility in land management applications, such as burn severity mapping, the focus of our study.

Burn severity mapping from remotely sensed imagery involves evaluating spectral reflectance characteristics of landscape features and relating that information to the severity of a fire. For example, in burned areas, increased bare ground area and decreased moisture elevates reflectance in mid-infrared spectral bands (Yool 1999), while a reduction in healthy vegetation “reduces near-infrared reflectance in direct relation to the intensity of the fire” (Jakubauskas *et al.* 1990). For Landsat Thematic Mapper imagery, Bands 4 and 7, are considered the wavelength ranges that, when combined in an index, best correspond to burn severity mapped on the ground (Key and Benson 2005a), though there is some dispute concerning the optimality of these bands for this application (Roy *et al.* 2006).

We selected a commonly used image-based methodology because our primary focus in this project was to assess the comparative utility of simulation modeling and a single satellite derived burn severity mapping approach. The Normalized Burn Ratio (NBR) is a linear combination of Landsat bands 4 and 7 calculated on single-date imagery. When NBR images are produced before and after a fire, the images can be differenced to enhance the contrast between pre and post-fire conditions, resulting in the Differenced Normalized Burn Ratio (Δ NBR) (Key and Benson, 2005b). We chose the Δ NBR as calculated from Landsat imagery as it seems to prevail in the literature as the most

commonly tested (and used) image-based severity mapping technique. The ΔNBR showed strong relationships with the Composite Burn Index (CBI), a field-based integrative assessment of burn severity (Cocke *et al.* 2005; Key and Benson, 2005a), and it was moderately correlated with a range of other field measured fire effects variables (Hudak *et al.* 2007). Landsat-based ΔNBR imagery related well in comparison with fine spectral resolution remote sensing methods of assessing burn severity (van Wagtenonk *et al.* 2004), and several other satellite image index methods of burn severity mapping (Brewer *et al.* 2005; Epting *et al.* 2005). The ΔNBR methodology has been used to map severity in a variety of ecosystems and landscapes across the United States (Duffy *et al.* 2007; Lentile *et al.* 2007) and internationally (Escuin, *et al.* 2008; but see Roy *et al.* 2006). ΔNBR is the landscape assessment methodology included in the FIREMON sampling protocol (Key and Benson 2005b), which is used in this study.

The ΔNBR approach is based on the observed changes in linear combinations of surface reflectance values between pre and post-fire images. Thus, it is essentially the *reflectance* of light from earth surfaces that is measured from date to date; image indices do not directly represent any biophysical process or fire effect. ΔNBR image values are dimensionless indices that can be sliced into categories to represent relative levels of fire severity (e.g. high, medium and low). This classification can facilitate a quick, simple and informative summary display of relative fire severity across the landscape. ΔNBR is also useful as a continuous variable, in which case each pixel has a unique, uncategorized value (Key and Benson 2005b).

Fire Effects Simulation Modeling

Computer models for predicting fire effects, such as FOFEM and CONSUME, have been available to fire management for over a decade (Keane *et al.* 1994; Ottmar *et al.* 1993). These models simulate the direct effects of a fire on the vegetation, fuels, and soils for a point in space and output these effects using biophysically based variables such as fuel consumption and tree mortality. Keane *et al.* (2009[in prep]) have implemented FOFEM into a spatial computer model called FIREHARM to develop spatially explicit maps of fire hazard and risk. FIREHARM can also simulate burn severity maps using the same methods used to predict fire hazard.

FIREHARM is a spatial model that simulates common measures of fire behavior, fire danger, and fire effects to use as variables to rate fire hazard, and then describes the distribution of these measures over multiple scales of time and space to estimate measures of fire risk by simulating weather and fuel moistures (Keane *et al.* 2009[in prep]). The fire effects predictions from FIREHARM can also provide important variables to describe burn severity physically. Simulated tree mortality, fuel consumption and soil heating estimates using wildfire fuel and weather conditions will allow the manager to fine tune management actions to specifically focus burned area rehabilitation efforts based on the type and extent of damage that has occurred. Users can also simulate best and worst case scenarios for possible situations that may occur in their region during the fire season, or they could use the model to guide the scheduling and location of fuels treatments. By modeling direct fire effects, burn severity assessments can be tailored for

specific management applications and maps could be produced anytime during a wildfire to provide instant assessments for real-time management of the fire.

FIREHARM requires several input data layers to compute spatial fire effects variables and burn severity. The most important of these for this study include digital maps of topography (elevation, aspect, slope), vegetation (tree attributes, cover type), and fuels (fuel loading) along with site-specific weather and fuel moisture estimates. These inputs are passed to the FOFEM model embedded in the FIREHARM program to generate estimates of tree mortality, fuel consumption, smoke emissions, and soil heating. While the FIREHARM model is equipped to calculate numerous fire behavior, fire danger and fire effects variables, for this study we will only use the fire effects output of fuel consumption and tree mortality.

Most of the FIREHARM input data will be available for the continental United States upon completion of the National LANDFIRE Mapping Project (www.landfire.gov). LANDFIRE is a multi-agency effort to provide land managers with comprehensive spatial data and planning-focused analysis tools. It will enable agencies to more efficiently and effectively manage their landscapes in accordance with the National Fire Plan (Rollins *et al.* 2003). In most cases, the effort required for managers to independently create the input data layers required to run FIREHARM would be cost, time, and resource prohibitive (Reinhardt *et al.* 2001). However, the availability of LANDFIRE data layers enables managers to run FIREHARM to generate fire hazard and burn severity maps, with relative ease.

Synergy of burn severity mapping approaches

Remotely sensed imagery and fire effects models provide extensive views of fire severity for large regions. Both technologies facilitate generation of quick and inexpensive maps, minimizing the need for resource-intensive and potentially dangerous field sampling. But, while they share some benefits and capabilities, these approaches differ greatly in process and product (Table 1). The FIREHARM modeling approach provides fire effects measurements in physical units, which are perhaps more meaningful, depending on the project objective, than a relative index of severity, which is what satellite images provide. However, both model and image data can be categorized into intuitive burn severity categories, if users need an integrated assessment. Both approaches can be used for rapid assessment situations, yet only FIREHARM has utility as a prognostic tool. Whereas FIREHARM input data will be consistent and accessible to users (most spatial layers have already been developed and archived for the nation by the LANDFIRE project), burn severity mapping using remote sensing is dictated by the availability of smoke and cloud-free imagery. Fire effects simulation approaches can generate fire severity maps in a shorter time (i.e., overnight) than remote sensing (i.e., sometimes weeks). Both methods require considerable analyst proficiency and significant computing resources to generate high quality burn severity maps.

Project Objectives

In this project, our objective was to compare and contrast the performance of model-based spatial fire effects and satellite-derived burn severity maps using field measured fire effects as validation. We investigated the possibility of combining these technologies to provide an optimal burn mapping system that integrates a biophysically-focused fire modeling approach and a satellite image-based view of burn severity. Pre-fire imagery and input data layers serve as the pre-fire data, while post-fire imagery and model output provide the means for fire effects evaluation.

Methods

This study compared burn severity image-based mapping and modeling approaches by implementing both for a set of wildfires that occurred in western Montana from 2003-2005. We list the following procedures as a general overview of the methods used in this comparison effort:

- *Sampled burned areas.* These field data were used to 1) quantify input variables for FIREHARM, 2) provide reference data for satellite imagery severity mapping, and 3) assess the accuracy of both simulation and imagery methods.
- *Gathered satellite burn severity maps.* Δ NBR imagery was generated by the Forest Service Remote Sensing Applications Center.

- *Simulated and mapped burn severity and fire effects.* We used FIREHARM for two different scenarios: 1) ‘Plot-based’ (parameterization using individual plots) and 2) ‘LANDFIRE-based’ (parameterization using LANDFIRE data).
- *Validated burn severity for imagery and FIREHARM methods.*
- *Compared both methods using accuracy assessments and lessons learned from the mapping process.*

Study Areas

We selected wildfire areas based on specific criteria. When we started the project, it was imperative that we collect data within LANDFIRE zones 19 or 16, as these were the zones that had a full set of data for model input. However, as our project progressed, full datasets became available for many other LANDFIRE zones. We first sampled the Zone 19 Cooney Ridge and Mineral Primm wildfires and then, once LANDFIRE completed Zone 10, we sampled the 2005 I90 Complex and the 2006 Gash Creek fires (fig. 1).

Though the four fires are located in two LANDFIRE zones, they are geographically close (all are within about 60km of Missoula, Montana, USA). Climate in these Northern Rocky Mountain landscapes is cool temperate, with a minor maritime influence. Mean annual temperature ranges from 2 to 8°C. Summers are dry and precipitation ranges from 410 to over 2,540 mm, with most falling as snow in spring, autumn and winter (McNab *et al.* 1994). The fires burned through varying topography (valleys, rolling foothills, steep sided ridges and peaks) ranging from 876 to 2,524 meters in elevation.

The Mineral Primm and Cooney Ridge fires started in early August of 2003 and each grew to over 10,000 ha by the time they were contained in mid September (Table 2). Vegetation cover in both fire areas is dominated by temperate coniferous forests and woodlands of Douglas-Fir (*Pseudotsuga menziesii*) (26% in Mineral Primm, 64% in Cooney Ridge), Engelmann spruce - subalpine fir (*Picea engelmannii* - *Abies lasiocarpa*) (26% in Mineral Primm, 11% in Cooney Ridge), and lodgepole pine (*Pinus contorta*) (15% in Mineral Primm, 7% in Cooney Ridge). The following cover types each comprise between 5% and 7% of the fire area landscapes: mesic montane meadows (tall forbs), deciduous shrublands and grassland/herbaceous cover types. Other less dominant cover types (each less than 1%) include sage (*Artemisia tridentata*) shrublands, and western larch (*Larix occidentalis*), ponderosa pine (*Pinus ponderosa*) and aspen (*Populus tremuloides*) forest types.

The I90 complex started on August 4, 2005 directly adjacent to Interstate 90, near the town of Alberton, Montana. The fire burned primarily through Douglas-fir dominated mixed conifer forests (41% of the fire landscape), grassland/herbaceous communities (28%), and ponderosa pine forests (13%). Each of the following cover types covered less than 3% of the burned area: Engelmann spruce–subalpine fir forests, lodgepole pine forests, sagebrush shrublands and riparian areas consisting primarily of cottonwood and willow. The final fire area at containment was reported as 4,452 ha.

The high elevation Gash Creek fire was ignited by lightning on July 24, 2006 in the northern Bitterroot Mountains near the town of Victor, MT. The fire grew to 3,561 ha

burning through landscapes dominated by mid to high elevation forest types: engelmann spruce–subalpine fir (46%), Douglas-fir (23%), whitebark pine (10%) and lodgepole pine forests (5%). Other cover types included grassland (5%), deciduous shrubland (3%) and ponderosa pine forest (1%). Approximately 3% of the area within the fire perimeter was non-vegetated.

Field Sampling

Since we could only sample fire effects after the wildfires had occurred, it was impossible to obtain a pre-fire fuel load for our fuel consumption calculations. Instead, we used a paired-plot approach where unburned plots were paired with adjacent burned plots that were similar in site characteristics (slope, aspect, elevation) and vegetation conditions (cover type, structural stage, fuel type) In a few cases, we were able to use a single unburned plot as a surrogate for multiple burned plots. Both natural features (topography, soil type and microclimate) and anthropogenic features (fire lines, roads, management units) combined to confound the search for potential plot sites within a homogenous fuel type that included both burned and unburned areas.

We used a 1049.79 m² (18.29 m radius) circular macroplot to define the sampling unit where we recorded plot description information, tallied trees and fuels for all burned and unburned plots, and assessed Composite Burn Index (CBI) only on burned plots . We followed FIREMON protocol (Lutes, et. al, 2005) for all field sampling. For trees, we recorded species, status (healthy, unhealthy, or dead), diameter at breast height (dbh)

(cm), tree height (m), crown class (open grown, emergent, dominant, codominant, intermediate or suppressed), char height (m), crown scorch (%) and noted snags (trees dead before the fire) for all dead mature trees (> 11.43 dbh) in the macroplot. Trees less than 11.43 dbh were counted as saplings and measured at the macroplot level. For saplings, we counted the number of trees in classes defined by species, dbh (cm) and average height (m). For seedlings (trees < 11.43 cm DBH, <1.37 m tall), we counted the number of trees in classes (defined the same as for saplings) in a 40.47 m² (3.59 m radius) microplot nested within the macroplot.

For fuel load sampling, we established as many sampling transects as needed to obtain 100 pieces of down woody debris; at minimum, we established three planes, oriented 90°, 300° and 270° true north following FIREMON protocols (Lutes *et al.* 2005). The sampling plane for 1-hour and 10-hour fuels extends 1.83 meters from the 3.05 meter mark of the tape, which has its origin at plot center. The sampling plane for 100-hour fuels extends 3.05 meters from the 3.05 meter mark of the tape. We counted pieces of each fuel component that crossed the tape and tallied these numbers in the plot sheets. For 1000-hour fuels, we tallied the diameter and rot condition (on a five level scale from sound to rotten) of every log over 7.62 cm in diameter for the entire length of the 18.29 meter tape. We estimated vegetation cover and height and took duff and litter depth measurements at the middle (9.14 meter mark) and the end (18.29 meter mark) of the tape.

Composite Burn Index (CBI), a ground-based burn severity measure designed to relate to the Δ NBR (Key and Benson 2005a), was assessed for all burned plots within the macroplot boundaries. The same field data were collected on burned and unburned plots, with additional sampling of CBI on burned plots only. We proposed to sample soil char depth and scorch height, but we found that it was too variable within a plot and too difficult to detect during our sampling.

Field data were entered into a FIREMON database, and fuel loading, tree mortality and CBI values were calculated and summarized for each plot. To calculate fuel consumption values for the field data, we simply subtracted fuel loads measured on burned plots from those measured on corresponding unburned plots. Tree mortality was calculated as the percentage of fire-killed dead trees on a plot. We used measures of fuel consumption and tree mortality as reference data in comparisons with model-derived and image-derived data.

Satellite Imagery

We obtained Burned Area Emergency Response (BAER) products for all four fires from the US Forest Service Remote Sensing Applications Center. They performed all of the necessary image preparation steps, such as pre and post-fire scene selection, radiometric and terrain correction and spatial co-registration (<http://www.fs.fed.us/eng/rsac/baer/>). The Normalized Burn Ratio (NBR) was calculated from pre and post-fire Landsat Thematic Mapper imagery as:

$$NBR_{Landsat} = \frac{Band4 - Band7}{Band4 + Band7}$$

Where Band 4 is the near infrared reflectance (0.76 – 0.90 μm) and Band 7 is the short wave infrared reflectance (2.08 – 2.35 μm). To capture fire-caused landscape change, (Key and Benson, 2005b) compute ΔNBR which is the difference between NBR from the pre-fire and post-fire scenes:

$$\Delta\text{NBR}_{Landsat} = \text{NBR}_{\text{prefire}} - \text{NBR}_{\text{postfire}}$$

The pre-fire scene was chosen from the year prior to the post-fire scene, ideally during a phenologically similar period. Our pre and post-fire image dates were mostly consistent with an “initial assessment” in which the pre-fire image is chosen from the year prior to the fire and the post-fire image is ideally selected directly following the fire (Key and Benson, 2005a). This image timing is consistent with our objective of testing a system for collecting and evaluating data immediately after a fire. One exception to this timing was that the pre-fire image for the I90 fire is from three years prior to the fire (Table 2) due to a lack of cloud-free pre-fire images in this area. We used the BARC256 product for our comparison because it represents ΔNBR as continuous variable, scaled such that values range from 0 to 256 with increasing burn severity. For the validation analysis, we used the continuous ΔNBR data, but to assess map agreement, we sliced the BARC256 into three classes to match the three FIREHARM burn severity classes using Jenks natural breaks (Jenks 1967).

FIREHARM Simulations

We used two FIREHARM simulation scenarios in this study. The ‘plot-based’ scenario was used both to *validate* FIREHARM and Δ NBR. It represents the most realistic evaluation of model capabilities, given the availability of accurate input information. We then included the ‘LANDFIRE-based’ scenario to *demonstrate* the landscape mapping capabilities and to replicate how FIREHARM would be used in operational settings without the availability of specific plot data for model parameterization.

Plot-based Simulations. For this scenario, we used the field data from each of the 64 plots in the four fire areas to parameterize FIREHARM explicitly for simulation of fire effects. We took the following inputs directly from the plot data forms: slope, aspect, elevation, vegetation type, and geographic position (latitude and longitude). Because the 40 model version of the Fire Behavior Fuel Models (Scott and Burgan 2005) was not available when we began our field sampling, we overlaid plot locations with LANDFIRE spatial data to obtain Fire Behavior Fuel Model values. We used the sampled tree information to create the tree list input to FIREHARM to calculate tree mortality (Keane et al. 2009[in prep]). The tree list requires the following fields: species, density (number of trees km⁻²), diameter at breast height (cm), tree height (m), canopy base height (m), crown class (open grown, emergent, dominant, codominant, intermediate or suppressed), and tree status (healthy, unhealthy, or dead). Since we wished to simulate tree mortality on our burned plots, we modified our collected data for burned plots to change the status of all trees that were killed by the fire from “dead” to “healthy”; snags (trees that were dead

before the fire), retained a “dead” status. Because we could not collect canopy base height information on the dead trees, we estimated this value as a function of tree height using FOFEM default values (Reinhardt et al. 1997). To parameterize pre-fire fuel loads, we used FIREMON data queries to calculate fuel loadings for each plot by sampled fuel components (1-hour, 10-hour, 100-hour, 1000-hour, litter and duff loads in kg m^{-2}) and used these values to populate a FIREHARM fuel loading input file.

For FIREHARM weather input, we gathered several types of weather and fuel moisture information during the burning period at our fire areas: 1) maximum temperature ($^{\circ}\text{C}$), 2) minimum temperature ($^{\circ}\text{C}$), 3) relative humidity (%), 4) wind speed (miles hr^{-1}), 5) wind direction (azimuth), fuel moistures for each fuel component. We accessed Kansas City Fire Access Software (KCFAS) through the National Fire and Aviation Management Web Access (FAMWEB) to obtain the necessary temperature, humidity, and wind information from weather stations at or near each of our four fire areas (Table 2). We then ran Fire Family Plus (Main *et al.* 1990) to estimate fuel moisture conditions for 1-hour, 10-hour, 100-hour, 1000-hour, herb and shrub components. We subjectively estimated live foliar moisture (set at 100%), litter moisture (set equal to 1-hour fuel moistures), and duff moisture (75%) as these values were not measured on our fires, nor are they products of National Fire Danger Rating System (NFDRS) (Burgan *et al.* 1977). We averaged the weather and fuels values through the record of the fire period (from ignition through containment) to obtain the single value (for each parameter) necessary to populate the weather and fuel moisture input file.

LANDFIRE-based Simulations. To demonstrate the rapid mapping capabilities of FIREHARM, the model was also parameterized with LANDFIRE spatial data. The following LANDFIRE layers from Zone 19 (for Cooney Ridge and Mineral Primm fires) and Zone 10 (for I90 and Gash Creek fires) were used as input: Existing Vegetation Type (EVT), Fire Behavior Fuel Model (FBFM), Fuel Loading Model (FLM), elevation, slope, and aspect (www.landfire.gov). Tree information came from a recently derived LANDFIRE tree list spatial data layer that summarizes tree information from all plots in the LANDFIRE reference database (Herynk et al. 2009[in prep]). We generated all other FIREHARM inputs (weather and fuel moisture) as described for the above plot validation parameterization.

We simulated and mapped three FIREHARM fire effects output variables for both parameterization scenarios in this study: 1) fuel consumption (a continuous variable reported as the percent of the pre-fire fuel load that is consumed), 2) tree mortality (a continuous variable reported as the percent of the total number of trees on a plot that died due to fire) and 3) burn severity, a categorical variable that integrates several fire effects factors. Keane *et al.* (2009[in prep]) compute fire severity based on classes of tree mortality (<40%, 40-70%, >70%), fuel consumption (<20%, 20-50%, >50%), and soil heating (<60 °C at 2 cm, 60-250 °C at 2 cm, >250 °C at 2 cm).

Comparison and Validation

We used the 64 extracted raster values (coincident with the plots) for both the validation of FIREHARM (plot-based and LANDFIRE-based scenarios) and Δ NBR, along with the CBI-based map accuracy assessments. For burn severity mapping and map agreement tables, we used the full set of pixels in the image or simulated rasters. Plot locations rarely fell directly in the center of a pixel, so when extracting Δ NBR and FIREHARM burn severity values for comparison with plot information we used a bilinear interpolation to obtain a distance-weighted average of the pixels adjacent to the plot-coincident pixel.

Results

Field Sampling

We sampled 23 unburned/burned plot pairs at Cooney Ridge, 28 at Mineral Primm, 8 at I90 and 5 at Gash Creek wildfire areas. The majority of the 64 plots pairs were located in forested vegetation types (49% Douglas-fir, 15% Engelmann spruce - subalpine fir, 7.5% lodgepole pine and 6% ponderosa pine) with fewer plots in grass (15%) and shrub (7.5%) cover types (Figure 2a). The plots were approximately normally distributed throughout the range of fire severity (Figure 2b). Though we originally intended to collect an equal number of plots in each of three burn severity classes (high, medium and low), the

limited extent of suitable area to install unburned/burned pairs dictated plot selection resulting in a low number of plots and uneven distribution across severity levels.

FIREHARM and Δ NBR Validation

We found a wide range in the strength of relationships between observed fuel consumption and simulated fuel consumption. Associations were generally stronger when the model was parameterized from our plot data ($r = 0.33$), than with the LANDFIRE-based scenario ($r = -0.06$) (Figure 3, a-c, Table 4). There was less disparity in relationship strength between parameterization scenarios for post-burn fuel load ($r = 0.51$ for individual plot-based, and $r = 0.44$ for LANDFIRE-based parameterizations). However, both parameterizations were comparable for the amount of fuel consumed, which was the variable with the strongest correlation between modeled and observed values, ($r = 0.92$ for plot-based and $r = 0.91$ for LANDFIRE-based parameterizations). In contrast, we found a very weak negative relationship between observed fuel consumption and Δ NBR ($r = -0.04$) (Figure 4).

The LANDFIRE-based FIREHARM simulations of percent tree mortality had a stronger relationship with observed tree mortality ($r = 0.37$) than did the plot-based parameterization ($r = 0.17$) (Figure 5). Tree mortality had a moderate positive correlation with Δ NBR ($r = 0.52$) (Figure 6). The tree mortality and fuel consumption predictions were used in the computation of simulated burn severity.

Burn severity mapping

Maps of Δ NBR, simulated fuel consumption, and simulated tree mortality exhibit markedly different spatial patterns across the landscape (Figure 7). When comparing categorized burn severity maps, it seems clear, visually, that Δ NBR and FIREHARM modeled burn severity maps vary in agreement between all four fires (Figure 8) (values range from 33.5% for the Cooney Ridge fire to 64.8% for Mineral Primm). Agreement values for Gash Creek and I90 Complex were intermediate at 63.9% and 48%, respectively (Table 5).

The FIREHARM burn severity maps are dominated by moderate severity predictions with user's accuracy high for this category (88.0%), but relatively low for the high and low burn severity classes (9.4 and 0.0%, respectively). This indicates that 88% of the time, a user will find that an area classified to the moderate burn severity category by both Δ NBR and FIREHARM burn severity map (Table 5). There is no agreement in the low category for Cooney Ridge because there were no pixels classified as low severity in the FIREHARM map.

We graphically compared the simulated tree mortality and fuel consumption to Δ NBR burn severity classes to evaluate if data points might cluster into zones of high, moderate and low severity based on fire effects across the full set of pixels in the wildfire area. For brevity, we present the results of this comparison for only the Cooney Ridge wildfire (Figure 9), which shows no discernable clusters of burn severity. We repeated this

analysis for our set of 64 points using the Composite Burn Index (rounded to the nearest integer) as a ground-measured indicator of burn severity (Figure 10). The individual plot parameterized simulation lacked a perceivable pattern of burn severity clusters, however it appears that the output of the LANDFIRE parameterized simulation produced enough separability to distinguish at least between the highest burn severity class and the two lower classes; the low and moderate classes appear to be indistinct from one another. When ΔNBR is plotted against FIREHARM-simulated fire effects variables, there appears to be a distinct cluster of high severity points (Figure 10). This is true for both of the simulation parameterization situations (LANDFIRE-based and plot-based) (Figure 10).

Accuracy assessment showed that ΔNBR and FIREHARM simulated burn severity maps had about the same level of overall agreement (57.8%) (Table 6). Agreement as measured by Kappa analysis for the ΔNBR map was poor ($\text{kappa} = 0.28, p = 0.003$). We could not calculate Kappa statistics for the FIREHARM burn severity map because there were no FIREHARM simulated plots classified in the low category.

Discussion

The main goal for this study was to demonstrate that image and model-derived burn mapping methodologies, used individually or in tandem, might have the potential to improve our ability to manage the effects of wildfires. It is clear that burn severity maps derived from these different technologies present managers a variety of alternatives. The

simulated burn severity maps provide a quick and comprehensive description of fire severity, but results can be suspect because of the low accuracy of the input layers, the complex nature of a spreading fire (see next section), and misrepresentation of weather and fuel conditions at the time of burn. On the other hand, satellite derived burn severity maps appear acceptable for describing cumulative fire effects over large areas, but the severity assessment 1) is not based on the physical measures of fire effects, 2) requires that an unobstructed image is available for the burned area and 3) cannot be produced to predict burn severity. Both approaches have distinct advantages and significant limitations (Table 1). It is interesting that when the model performed poorly (predicting tree mortality), the imagery performed relatively well, and where the model performed relatively well (predicting fuel consumption), the imagery performed poorly (Table 5). Our preliminary results indicate that there may be differing capabilities in the assessment of fire effects using a simulation model versus using satellite imagery and that the two used together could perhaps provide a more comprehensive burn severity map product.

Map agreement between the Δ NBR and FIREHARM burn severity maps is most influenced by the large areas of moderate severity in the FIREHARM maps (Figure 8; Tables 5 and 6) which may boost the overall map agreement and lower the user's accuracy (Table 5). In the case of the Cooney Ridge fire, Δ NBR shows a large area of low severity that is classified as moderate severity by FIREHARM (Figure 8). It may be that the fire severity key in Keane et al [2009 in prep] does not perform well for low severity fires.

It is encouraging that under both FIREHARM parameterization scenarios, the combination of Δ NBR and simulated fire effects variables seem to cluster into somewhat discernable burn severity classes. These findings suggest that the two systems might be paired to improve evaluations of fire effects, especially since neither is obviously superior in terms of accuracy (Table 6) or utility (Table 1). Moreover, results for the LANDFIRE-parameterized simulation showed discernable Δ NBR burn severity clusters in plots of fuel consumption and tree mortality (Figure 10), which shows potential utility of the model in cases in where satellite imagery is not available and the utility of the model to provide context to imagery classified burn severity.

The comparison of Composite Burn Index (CBI) to Δ NBR and FIREHARM burn severity is really not a true evaluation of accuracy. CBI is a standardized method that was designed to provide a severity context in which to interpret Δ NBR (Key and Benson 2006a). It is based on a number of visual and structural characteristics that may or may not be related to fire effects. The fire severity index as computed in FIREHARM, on the other hand, is based on the simulated tree mortality and fuel consumption. As a result, the three ordinal categories of the CBI, Δ NBR burn severity, and FIREHARM fire severity are not directly comparable so we could not perform a consistent accuracy assessment. However, we feel the comparison provides important information regarding the performance of each map product.

We suspect that the low Kappa score for our assessment of agreement between CBI and Δ NBR may be due to 1) the low total number of field plots that we sampled, and 2)

uneven plot distribution through the range of severity. Other studies found stronger agreements between CBI and Landsat-based assessments of burn severity: Cocke *et al.* (2005) sampled 92 plots and obtained Kappa values of 0.66 and 0.62 for Δ NBR maps from two different years, Miller and Thode (2007) used 741 CBI plots in an accuracy assessment of a relativized Δ NBR ($\kappa = 0.42$).

The strong performance by FIREHARM in predicting fuel consumption is partially due to our ability to parameterize the model's fuel module with actual plot data. Data with this level of detail may be difficult to obtain by the average user, who often resorts to using LANDFIRE fuel loading model data to parameterize the FIREHARM. Our results show that the coarse scale of the LANDFIRE inputs would likely introduce additional error in model predictions, because fuel loadings are more highly variable.

Correspondingly, our fuel loading results would likely have been even stronger had we been able to measure actual pre-fire loadings, instead of using a similar plot as a pre-fire surrogate. We suspected that using this paired plot approach would contribute error to our field-based fuel consumption estimates and this would consequently effect the degree of association between ground reference with modeled and satellite burn severity estimates, but there was no alternative fuel sampling methodology. Another source of error is our inability to capture fire spread and fuel dynamics due to the incompatible sampling scale.

The prediction of FIREHARM simulated tree mortality as calculated with field data or LANDFIRE products has a number of potential limitations:

- *Fire intensity.* FIREHARM predicts fire behavior assuming a heading fire, which results in increased tree mortality. The dynamics of flanking, or backing fires (which occur on natural landscapes) are not captured in the model and this explains why the model often predicts 100% tree mortality.
- *Scorch height.* FIREHARM uses one measure of scorch height for the entire pixel whereas real fires tend to have high variability in scorch height within a small area. This affects the ability of the model to predict whether a crown fire occurs, and if so, what type of fire behavior will result (running or dependent).
- *Weather information.* In some cases, the weather stations that we used to estimate fuel moisture inputs were distant from the fire (up to 25 km). We suspect that predictions may have been better if weather were available at a fine spatial scale.
- *Fuels.* Fuel loadings and characteristics vary at finer scales than both the plot measurements and the LANDFIRE mapping products.
- *Paired plot approach.* Pre-fire fuel conditions of burned areas may not have been fully represented by sampling an adjacent unburned area.

We believe that the coarseness of the input data and the generality of some of the model algorithms (Keane et al. 2009[in prep]) precludes our modeling efforts from thoroughly capturing fine scale variability of fire effects to create highly accurate burn severity maps, though we are encouraged by strong correlations between observed and simulated fuel consumption.

Considering satellite-sensor-target relationships, the low correlation between ΔNBR imagery and fuel consumption and the relatively high correlation between ΔNBR and tree

mortality is not surprising. It makes intuitive sense that a satellite image would do a better job of capturing the dynamics of the overstory (first layer of material “seen” by the sensor) than the understory that is obscured by this top layer. This is consistent with Epting *et al.* (2005), who found imagery was highly correlated to burn severity in only forested cover types, and Hudak *et al.* (2007), who found overstory measures of canopy closure were more highly correlated to imagery than understory measures.

We feel that both satellite imagery and modeling approaches have great value to fire management depending on time, place, resources, and available data (Table 1). Real time assessments of fire effects can be successfully accomplished using a modeling approach whereas long-term severity assessments for rehabilitation efforts could use the imagery data. Imagery data can also be combined with the simulated results to provide a physical basis for understanding and interpreting patterns of severity. For example, Δ NBR maps could be overlaid with predicted fuel consumption and tree mortality maps to develop Δ NBR thresholds to delineate burn severity classes in the absence of field data. Moreover, burn severity from imagery could be cross-referenced with predicted fire effects to tailor the burn severity for a specific management application. The Δ NBR maps, for example, can be cross-referenced with FIREHARM output to determine areas of high tree mortality and deep soil heating. Neither approach has the high accuracy that would suit all the multifaceted needs desired by fire and land management, but the integration of both approaches may lead to a synergy in the understanding and assessment of fire severity, especially as more comprehensive data and more accurate fire effects models become available in the future.

We envision that fire managers could use this technology in real-time wildfire operational assessments and immediate post-wildfire rehabilitation planning. Burn severity maps of burned and un-burned areas can be created by FIREHARM very quickly (overnight) using LANDFIRE data. These maps can be used to evaluate the benefits of allowing the fire to burn or the drawbacks of trying to put it out. We are currently developing a software tool that will use these simulated burn severity maps to compute the departure from historical severities. As satellite or air-borne images become available, image-derived burn severity maps can be integrated with simulated fire effects maps to design wildfire remediation plans and implement rehabilitation efforts. An integrated simulated- Δ NBR burn severity map could then be used to update existing GIS layers of vegetation, fuels, and other associated characteristics.

Acknowledgements

This effort was funded by the Joint Fire Sciences Program Agreement 05-1-1-12. We thank Jason Herynk, of Systems for Environmental Management, and Stacy Drury, Rocky Mountain Research Station, Missoula Fire Sciences Laboratory.

References

Anderson HE (1982) 'Aids to determining fuel models for estimating fire behavior'.
USDA Forest Service Rocky Mountain Research Station General Technical
Report RMRS-GTR-122. (Ogden, UT)

- Bigler C, Kulakowski D, Veblen TT (2005) Multiple disturbance interactions and drought influence fire severity in Rocky Mountain subalpine forests. *Ecology* 86(11), 3018-3029.
- Brennan MW, Hardwick PE (1999) Burned Area Emergency Rehabilitation teams utilize GIS and remote sensing. *Earth Observation Magazine* 8(6), 14-16.
- Brewer CK, Winne JC, Redmond RL, Opitz DW, Mangrich MV (2005) Classifying and mapping wildfire severity: a comparison of methods. *Photogrammetric Engineering and Remote Sensing* 71(11), 1311-1320.
- Burgan RE (1979) 'Estimating live fuel moisture for the 1978 National Fire Danger Rating System'. USDA Forest Service, Intermountain Forest and Range Experiment Station General Technical Report INT-167. (Ogden, UT)
- Campbell J (1996) 'Introduction to remote sensing.' (The Guilford Press: New York)
- Chuvieco E (1999) Measuring changes in landscape pattern from satellite images: short-term effects of fire on spatial diversity. *International Journal of Remote Sensing* 20(12), 2331-2346.
- Cocke AE, Fule, PZ Crouse JE (2005) Comparison of burn severity assessments using Differenced Normalized Burn Ratio and ground data. *International Journal of Wildland Fire* 14, 189-198.
- Diaz-Delgado R, Lloret F, Pons X (2003) Influence of fire severity on plant regeneration by means of remote sensing imagery. *International Journal of Remote Sensing* 24(8), 1751-1763.

- Duffy PA, Epting J, Graham JM, Rupp TS, McGuire DA (2007) Analysis of Alaskan burn severity patterns using remotely sensed data. *International Journal of Wildland Fire* **16**(3), 277-284.
- Epting J, Verbyla D, Sorbel B (2005) Evaluation of remotely sensed indices for assessing burn severity in interior Alaska using Landsat TM and ETM+. *Remote Sensing of Environment* **96**, 328-339.
- Eidenshink J, Schwind B, Brewer K, Zhu Z, Quayle B, Howard S (2007) A project for monitoring trends in burn severity. *Fire Ecology* **3**(1), 3-21.
- Escuin S, Navarro R and Fernandez P (2008) Fire severity assessment using NBR (Normalized Burn Ratio) derived from LANDSAT TM/ETM images. *International Journal of Remote Sensing* **29**(4), 1053-1073.
- Ferry GW, Clark RG, Montgomery RE, Mutch RW, Leenhouts WP, Zimmerman GT (1995) 'Altered fire regimes within fire-adapted ecosystems.' In 'Our living resources' (Eds ET LaRoe, GS Farris, CE Puckett, PD Doran, MJ Mac). U.S. Department of the Interior, National Biological Service. (Washington, D.C.)
- Hammill KA, Bradstock RA (2006) Remote sensing of fire severity in the Blue Mountains: influence of vegetation type and inferring fire intensity. *International Journal of Wildland Fire* **15**, 213-226.
- Hardwick PE, Lachowski H, Griffith R, Parsons A (1998) Burned area emergency rehabilitation project: an example of successful technology transfer. In 'Proceedings of the Seventh Forest Service Remote Sensing Applications Conference, 6-10 April 1998, Nassau Bay, Texas'. (Ed. JD Greer) pp. 62-71. American Society for Photogrammetry and Remote Sensing.

- Herynk J, in prep. LANDFIRE Tree List.
- Hudak AT, Morgan P, Bobbit MJ, Smith AMS, Lewis SA, Lentile LB, Robichaud PR, Clark JT, McKinley RA (2007). The relationship of multispectral satellite imagery to immediate fire effects. *Fire Ecology* **3**(1), 64-90.
- Jakubauskas ME, Lulla KP, Mausel PW (1990) Assessment of vegetation change in a fire-altered forest landscape. *Photogrammetric Engineering and Remote Sensing* **56**(3), 371-377.
- Jenks GF (1967) The Data Model Concept in Statistical Mapping. *International Yearbook of Cartography* **7**, 186-190.
- Keane RE, Reinhardt E (1994). FOFEM -- A First Order Fire Effects Model for predicting the immediate consequences of wildland fire in the United States. In Proceedings of the 12th Conference of Fire and Forest Meteorology, October 26-28, 1993 (Jekyll Island, GA).
- Keane RE, Veblen T, Ryan KC, Logan J, Allen C, Hawkes B (2002) The cascading effects of fire exclusion in the Rocky Mountains. In 'Rocky Mountain Futures: An Ecological Perspective'. (Ed. JS Baron) pp. 133-153. (Island Press: Washington DC, USA)
- Keane RE, in prep. FIREHARM demonstration and user's guide.
- Key CH, Benson NC (2005a). Landscape Assessment: Remote sensing of Severity, the Composite Burn Index. In 'FIREMON: Fire Effects Monitoring and Inventory System.' (Eds DC Lutes, RE Keane, JF Caratti, CH Key, NC Benson, LJ Gangi) USDA Forest Service, Rocky Mountain Research Station General Technical Report RMRS-GTR-164 (Ogden, UT)

- Key CH, Benson NC (2005b). Landscape Assessment: Remote sensing of Severity, the Normalized Burn Ratio. In 'FIREMON: Fire Effects Monitoring and Inventory System.' (Eds DC Lutes, RE Keane, JF Caratti, CH Key, NC Benson, LJ Gangi) USDA Forest Service, Rocky Mountain Research Station General Technical Report RMRS-GTR-164 (Ogden, UT)
- Kotliar NB, Simonson S, Chong G, Theobald D (2003) Effects on species of concern. In 'Hayman Fire Case Study'. (Ed RT Graham) USDA Forest Service, Rocky Mountain Research Station General Technical Report RMRS-GTR-114. (Ogden, UT)
- Kushla JD, Ripple WJ (1998) Assessing wildfire effects with Landsat thematic mapper data. *International Journal of Remote Sensing* **19**(13), 2493-2507.
- Lachowski H, Hardwick P, Griffith R, Parsons A, Warbington R (1997) Faster, better, data for burned watersheds needing emergency rehab. *Journal of Forestry* **95**, 4-8.
- Lentile LB, Holden ZA, Smith AM, Falkowski MJ, Hudak AT, Morgan P, Lewis SA, Gessler PE, Benson NC (2006). Remote sensing techniques to assess active fire characteristics and post-fire effects. *International Journal of Wildland Fire* **15**, 319-345.
- Lentile, LB, Morgan P, Hudak AT, Bobbit MJ, Lewis SA, Smith AMS, Robichaud PR (2007). Post-fire burn severity and vegetation response following eight large wildfires across the western United States. *Fire Ecology* **3**(1), 91-101.
- Lopez Garcia MJ, Caselles V (1991) Mapping burns and natural reforestation using Thematic Mapper data. *Geocarto International* **6**, 31-37.

- Lutes DC, Keane RE, Caratti JF, Key CH, Benson NC, and Gangi LJ (Eds), 2006. 'FIREMON: Fire Effects Monitoring and Inventory System'. USDA Forest Service, Rocky Mountain Research Station General Technical Report RMRS-GTR-164 (Fort Collins, CO)
- Main WA, Paananen DM, Burgan RE (1990) 'Fire Family Plus'. USDA Forest Service North Central Forest Experiment Station General Technical Report NC-138. (St. Paul, MN)
- McNab WH, Avers PE (Comps) (1994) 'Ecological Subregions of the United States: Section Descriptions'. 267 pp. USDA Forest Service Administrative Publication WO-WSA-5. Eco-system Management. (Washington, D.C.)
- Miller JD, Yool SR (2002) Mapping forest post-fire canopy consumption in several overstory types using multi-temporal Landsat TM and ETM data. *Remote Sensing of Environment* **82**, 481-496.
- Miller JD, Thode AE (2007) Quantifying burn severity in a heterogeneous landscape with a relative version of the Normalized Burn Ratio (dNBR). *Remote Sensing of Environment* **109**, 66-80.
- Morgan PE, Hardy CC, Swetnam TW, Rollins MG, Long DG (2001) Mapping fire regimes across time and space: Understanding coarse and fine-scale fire patterns. *International Journal of Wildland Fire* **10**, 329-342.
- NWCG (National Wildfire Coordinating Group) (2003) Interagency Strategy for the Implementation of Federal Wildland Fire Management Policy.
http://www.nifc.gov/fire_policy/pdf/strategy.pdf

- Ottmar RD, Burns MF, Hall JN, Hanson AD (1993) 'CONSUME users guide'. USDA Forest Service General Technical Report Pacific Northwest Research Station GTR-PNW-304. (Portland, OR)
- Pratt S, Holsinger L, Keane RE (2006). Using simulation modeling to assess historical reference conditions for vegetation and fire regimes for the LANDFIRE prototype project. In 'The LANDFIRE Prototype Project: nationally consistent and locally relevant geospatial data for wildland fire management.' (Eds MG Rollins, CK Frame) USDA Forest Service, Rocky Mountain Research Station General Technical Report RMRS-GTR-175. (Fort Collins, CO)
- Reinhardt ED, Keane RE, Brown JK (1997) 'First Order Fire Effects Model: FOFEM 4.0 User's Guide.' USDA Forest Service, Intermountain Research Station General Technical Report INT-GTR-344. (Ogden, UT)
- Reinhardt ED, Keane RE, Brown, JK (2001) Modeling Fire Effects. *International Journal of Wildland Fire* **10**, 373-380.
- Rollins MG, Keane RE, Zhu Z, Menakis JP (2006) An overview of the LANDFIRE Prototype Project. In 'The LANDFIRE Prototype Project: nationally consistent and locally relevant geospatial data for wildland fire management.' (Eds MG Rollins, CK Frame) USDA Forest Service, Rocky Mountain Research Station General Technical Report RMRS-GTR-175. (Fort Collins, CO)

- Roy DP, Boschetti L, Trigg SN (2006) Remote sensing of fire severity: Assessing the performance of the Normalized Burn Ratio. *IEEE Geoscience and Remote Sensing Letters* **3**(1), 112-116.
- Ryan KC, NV Noste (1985) Evaluating prescribed fires. P. 230-238 In 'Proceedings, symposium and workshop on wilderness fire.' (Eds JE Lotan, BM Kilgore, WC Fischer and RM Mutch) USDA Forest Service, Intermountain Research Station General Technical Report INT-182. Ogden, UT.
- Scott JH, Burgan RE (2005) 'Standard fire behavior fuel models: a comprehensive set for use with Rothermel's surface fire spread model.' USDA Forest Service, Rocky Mountain Research Station General Technical Report RMRS-GTR-153. Fort Collins, CO.
- Sunar F, Ozkan C (2001) Forest fire analysis with remote sensing data. *International Journal of Wildland Fire* **22**(12), 2265-2277.
- Turner MG, Hargrove WW, Gardner RH, Romme WH (1994) Effects of fire on landscape heterogeneity in Yellowstone National Park, Wyoming. *Journal of Vegetation Science* **5**, 731-742.
- Turner MG, Romme WH, Gardner RH (1999) Prefire heterogeneity, fire severity, and early post-fire plant reestablishment in subalpine forests of Yellowstone National Park, Wyoming. *International Journal of Wildland Fire* **9**(1), 21-36.
- USFS (1995) Burned Area Rehabilitation Handbook. USDA Forest Service Handbook 2509.13, Amendment No. 2509.13-95-7. (Washington DC)

- van Wagtendonk JW, Root RR, Key CH (2004) Comparison of AVIRIS and Landsat ETM+ detection capabilities for burn severity. *Remote Sensing of Environment* **92**, 397-408.
- Verbyla DL (1995) 'Satellite remote sensing of natural resources'. (CRC Press: Boca Raton)
- White JD, Ryan KC, Key CC, Running SW (1996) Remote Sensing of Forest Fire Severity and Vegetation Recovery. *International Journal of Wildland Fire* **6**(3), 125-136.
- Yool SR (1999) Remote Sensing Fire Studies in the Greater Borderlands. In 'Toward Integrated Research, land management, and ecosystem protection in the Malpai borderlands: conference summary.' 6-8 January 1999, Douglas, Arizona. USDA Forest Service Rocky Mountain Research Station Proceedings p-10. (Fort Collins, CO)
- Zarriello TJ, Knick ST, Rotenberry JT (1995) Producing a burn/disturbance map for the Snake River Birds of Prey National Conservation Area. In 'Snake River birds of prey national conservation area research and monitoring annual report.' USDOI Bureau of Land Management. (Boise, ID)

Tables

Table 1. Qualitative comparison of model-based and imagery-based burn mapping methods.

	Fire Effects Modeling (FIREHARM)	Remotely Sensed Imagery (ΔNBR)
Fire effects estimation	Provides biophysically based fire effects estimates.	Typically categorized into severity classes using subjectively chosen thresholds. As an index, it does not directly provide information about biophysical processes or first order fire effects.
Burn Severity Maps	Can map fire effects variables (continuous or classed) and can output a thematic burn severity map.	Imagery can be displayed as the continuous range of the index or classed into severity categories.
Rapid assessment	Can provide severity maps for operational, real-time use at any time or location.	In some cases, imagery is immediately available post-fire, facilitating an instantaneous Δ NBR assessment, and timely burned area rehabilitation
Predictive Capabilities	Could be used as a predictive tool, with fire hazard and risk mapping capabilities.	Must be calculated after the fire has occurred and an image is available. It cannot be used as a predictive tool.
Data Archive	Model data can be generated in any volume at any time, given analyst and input data availability.	Archived burn severity data will be readily available from the Monitoring Trends in Burn Severity Project (Extended Assessment only).
System Availability	Most simulation models are in the public domain, so users incur no software cost. Most spatial input data will be free and available from LANDFIRE.	Due to instrument malfunction, timing of satellite overpass, or smoke/cloud obstruction, imagery may be unavailable or unacceptable at the time it is critically needed.
Data Preparation	Pre-fire weather and fuel moisture information must be collected or calculated, and various topographic and ecophysiological data layers must be developed in order to run the model.	Many steps are involved in the creation of a Δ NBR image from initial scene acquisition, through image processing and final image classification.
Data Quality	FIREHARM output quality depends on input data accuracy and model algorithm reliability.	Image quality is seasonally affected by sun angles and terrain shadows, which complicate image interpretation.
User Resource Requirements	Significant computing resources (memory and processor speed) are necessary to run FIREHARM for large landscapes. GIS software is required for input preparation and output display. FIREHARM analyst must be familiar with fire effects simulation modeling and GIS data management.	Significant computing resources (memory and processor speed) are necessary to store and manage satellite imagery. GIS and image analysis software is necessary for data preparation and image display. Image analyst must be familiar with satellite and GIS data management.

Table 2. Important information for the wildfires used in this study

Fire	Cooney Ridge	Mineral Primm	I90 Complex	Gash Creek
Approximate Start Date*	8-AUG-03	6-AUG-03	4-AUG-05	24-JUL-06
Approximate Containment Date*	15-SEP-03	19-SEP-03	21-AUG-05	16-SEP-06
Approximate Location	18 km E of Florence	31 km NE of Missoula	North of I90, near Alberton	10 km SW of Victor
Size at containment (ha)*	10,392	10,199	4,452	3,561
Cause*	Lightning	Unknown	Unknown	Lightning
Fuel Models*¹	5, 10, 12, 13	10	2, 13	10
Weather Station (Name and Location)	Stevensville 46° 30' 43" -114° 5' 33"	Point Six 47° 2' 28" -113° 58' 45"	Ninemile 47° 18' 39" -114° 24' 8"	Smith Creek 46° 27' 2" -114° 15' 10"
Pre-fire ΔNBR Image Date	10-JUL-2002	10-JUL-2002	10-JUL-2002	11-AUG-2005
Post-fire ΔNBR Image Date	31-AUG-2003	31-AUG-2003	19-AUG-2005	01-SEP-2006

*From National Incident Management Coordination Center Incident Management Situation Reports.

¹Fuel models are described in Anderson, et al. (1982).

Table 3. FIREHARM weather and fuel moisture input values

	Cooney Ridge	Mineral Primm	I90 Complex	Gash Creek
Min. Temperature (°C)	26.6	28.3	30.6	23.4
Max. Temperature (°C)	11.0	7.2	8.8	10.9
Relative Humidity (%)	35	29	23	33
Wind Speed (km hr⁻¹)	6	11	10	6
Wind Direction (azimuth)	237	180	180	90
1 hour FM (%)	5	6	4	6
10 hour FM (%)	6	10	5	7
100 hour FM (%)	12	13	9	8
1000 hour FM (%)	12	14	10	13
10,000 hour FM (%)	0	0	0	0
Foliar Moisture (%)	100	100	100	100
Litter Moisture (%)	5	6	4	6
Duff Moisture (%)	75	75	75	75
Herbaceous Moisture (%)	65	79	41	66
Shrub Moisture (%)	88	107	72	97

Table 4. Pearson correlations between modeled fire effects and observed fire effects for simulations with specific plot parameterization (first column), for simulations parameterized with LANDFIRE data (second column) and between Δ NBR and observed fire effects (third column). Values in bold are significant ($p < 0.01$).

	FIREHARM Individual Plot Parameterization	FIREHARM LANDFIRE Parameterization	ΔNBR
Amount of Fuel Consumed	0.92	0.91	-
Post-burn fuel load	0.51	0.44	-
Fuel Consumption	0.33	-0.06	-0.04
Tree Mortality	0.18	0.37	0.53

Table 5. Crosstabulation of Δ NBR classified data (columns) vs. FIREHARM burn severity classified data (rows) for the four wildfire areas. Cell values represent area (ha) that is classified for both maps.

	Low	Moderate	High	Total	<i>User's Accuracy (%)</i>
Cooney Ridge					
Low	0.00	3503.34	297.54	3800.9	0.0
Moderate	0.00	3287.70	447.93	3735.6	88.0
High	0.00	2874.33	297.54	3171.9	9.4
Total	0.0	9665.4	1043.0	10708.4	
<i>Producer's Accuracy (%)</i>	0.0	36.2	28.5		33.5
Mineral Primm					
Low	0.2	546.1	12.6	558.9	0.0
Moderate	5.5	6038.7	186.1	6230.3	96.9
High	3.2	2571.9	85.3	2660.4	3.2
Total	8.9	9156.7	284.0	9449.5	
<i>Producer's Accuracy (%)</i>	2.0	6.0	4.4		64.8
Gash Creek					
Low	38.4	185.1	2.8	226.3	17.0
Moderate	58.6	1997.8	51.5	2107.8	94.8
High	1.2	866.1	24.2	891.5	2.7
Total	98.2	3049.0	78.5	3225.6	
<i>Producer's Accuracy (%)</i>	39.2	6.1	3.5		63.9
I90 Complex					
Low	0.1	786.4	81.5	868.0	0.0
Moderate	0.0	1993.5	239.7	2233.2	89.3
High	0.0	1300.9	237.5	1538.3	15.4
Total	0.1	4080.8	558.7	4639.6	
<i>Producer's Accuracy (%)</i>	100.0	19.3	14.6		48.1

Table 6. Crosstabulation of CBI (columns) and classified burn severity maps (rows) for the 64 plots.

	Low	Moderate	High	Total	<i>User's Accuracy (%)</i>
ΔNBR					
Low	2	7	0	9	22.2
Moderate	3	20	6	29	69.0
High	0	11	15	26	57.7
Total	5	38	21	64	
<i>Producer's Accuracy (%)</i>	40.0	52.6	71.4		57.8
FIREHARM					
Low	0	0	0	0	0.0
Moderate	4	33	17	54	61.1
High	1	5	4	10	40.0
Total	5	38	21	64	
<i>Producer's Accuracy (%)</i>	0.0	86.8	19.0		57.8

Figures

Figure 1. Map of study areas showing LANDFIRE zones, wildfires (in red) and plot locations (green points).

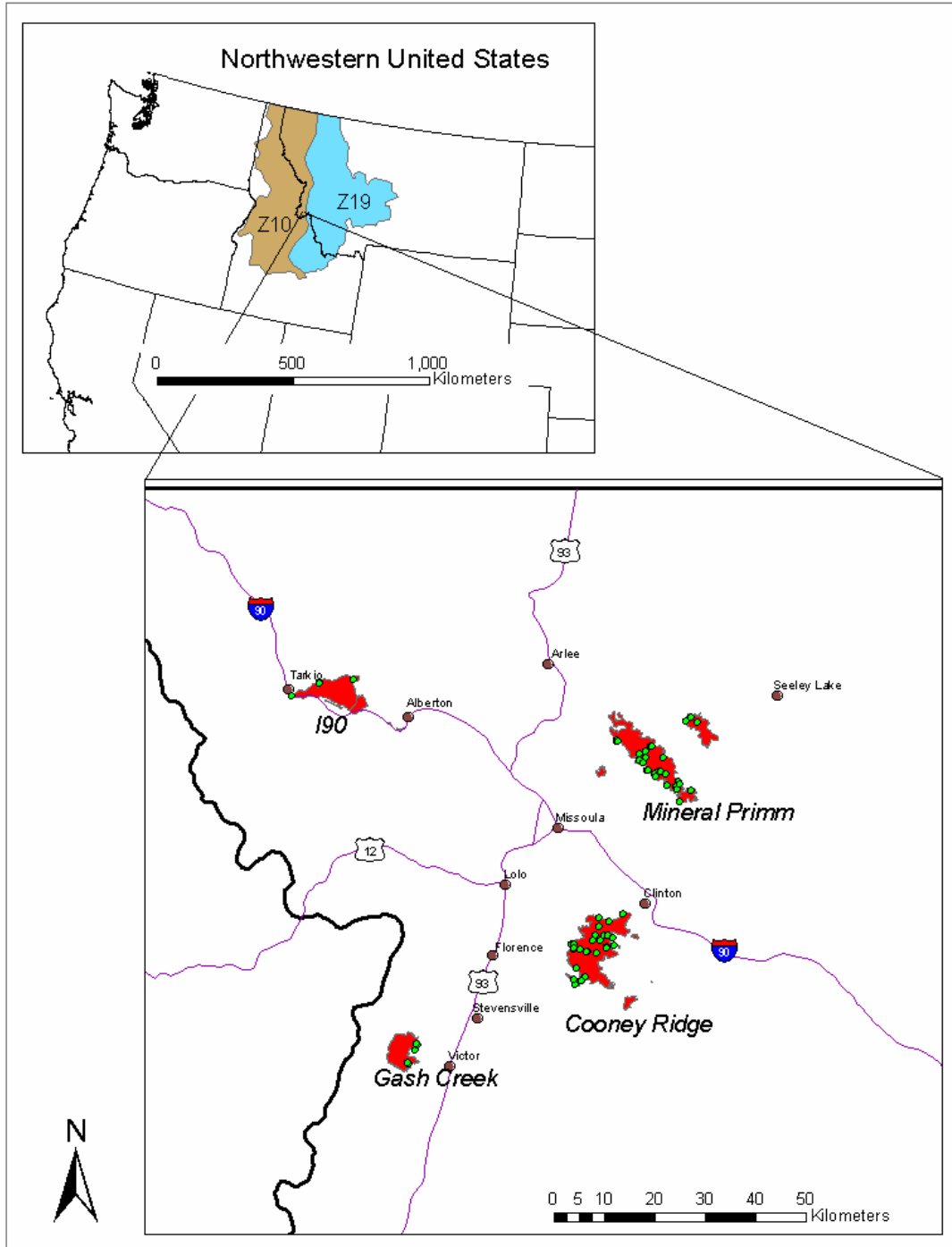


Figure 2. Distribution of the 64 plots collected in the four wildfire areas across (A) vegetation types and (B) Composite Burn Index (CBI) scores.

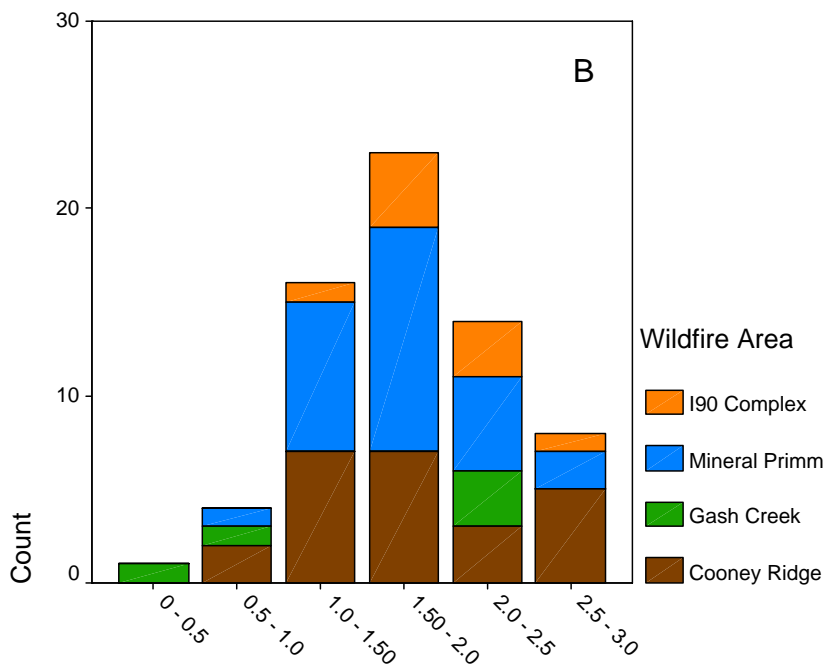
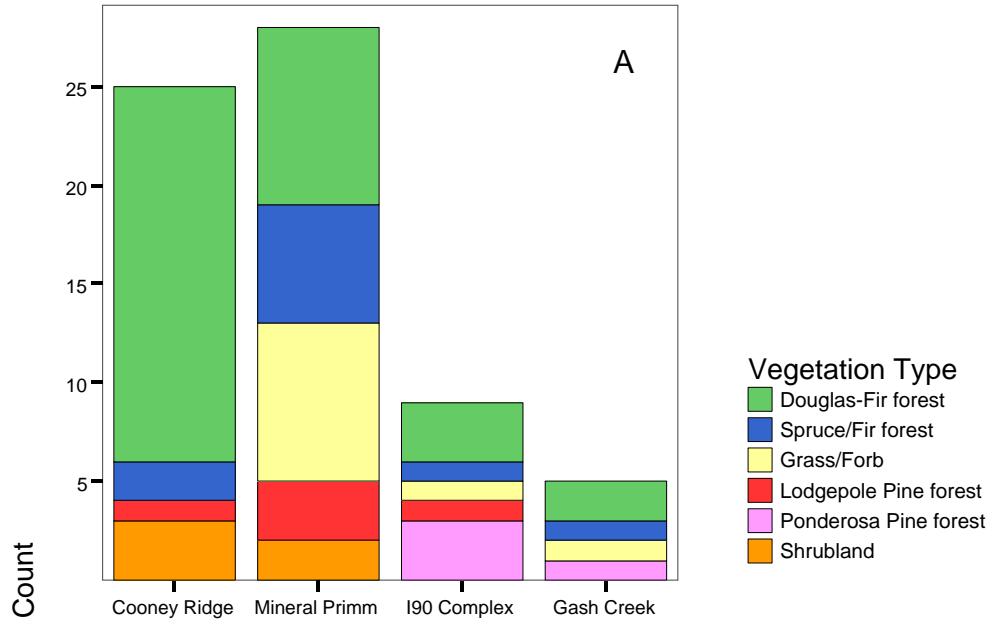
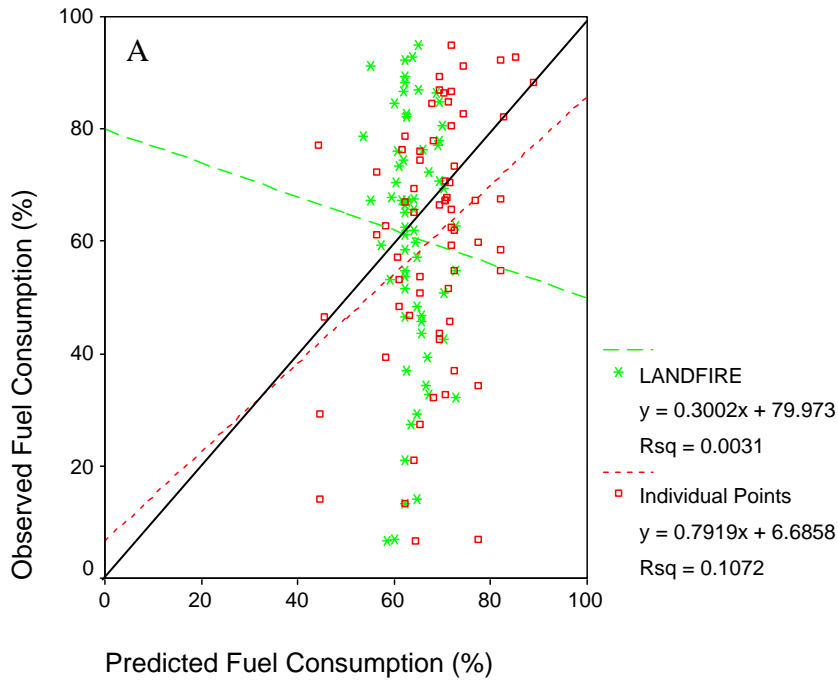


Figure 3. Relationship between observed and predicted fuel consumption variables: A. fuel consumption (%). B. Post-burn fuel load (kg m⁻²), C. Amount of fuel consumed (kg m⁻²). The large dash and small dash lines represent the regression trend lines for the FIREHARM simulations using LANDFIRE-parameterized and individually-parameterized data respectively. The solid black line is a 1:1 line.



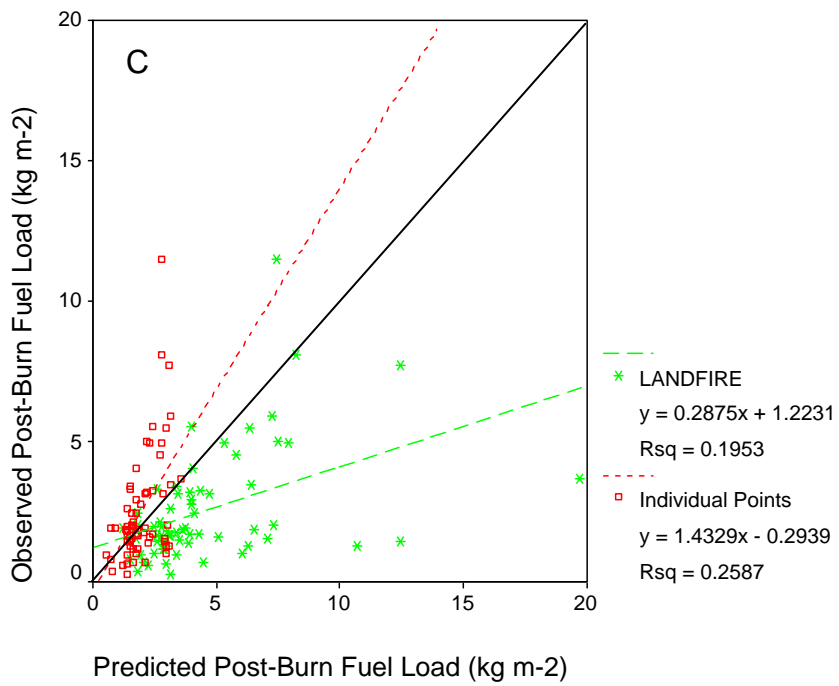
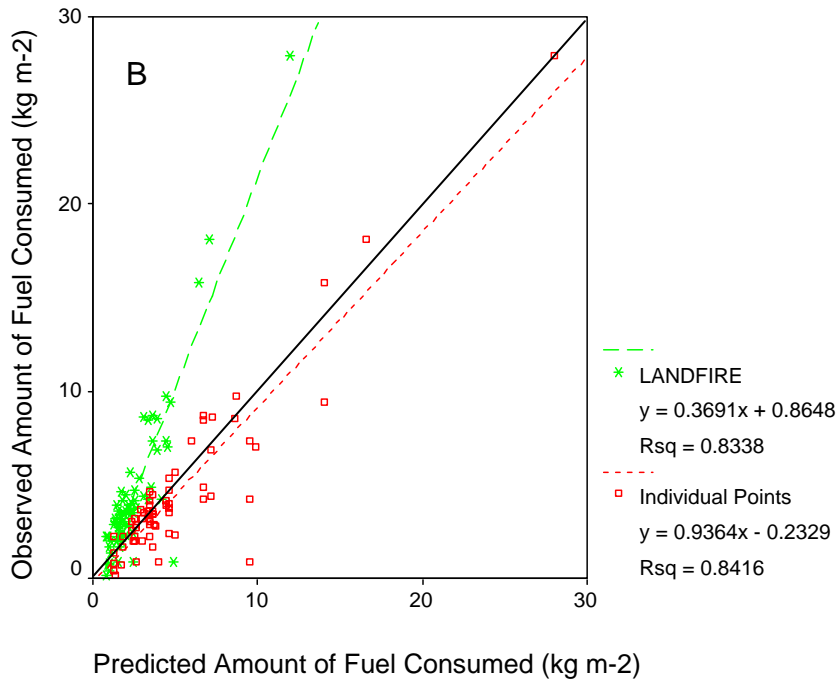


Figure 4. Lack of relationship between observed fuel consumption (%) and the Differenced Normalized Burn Ratio (Δ NBR).

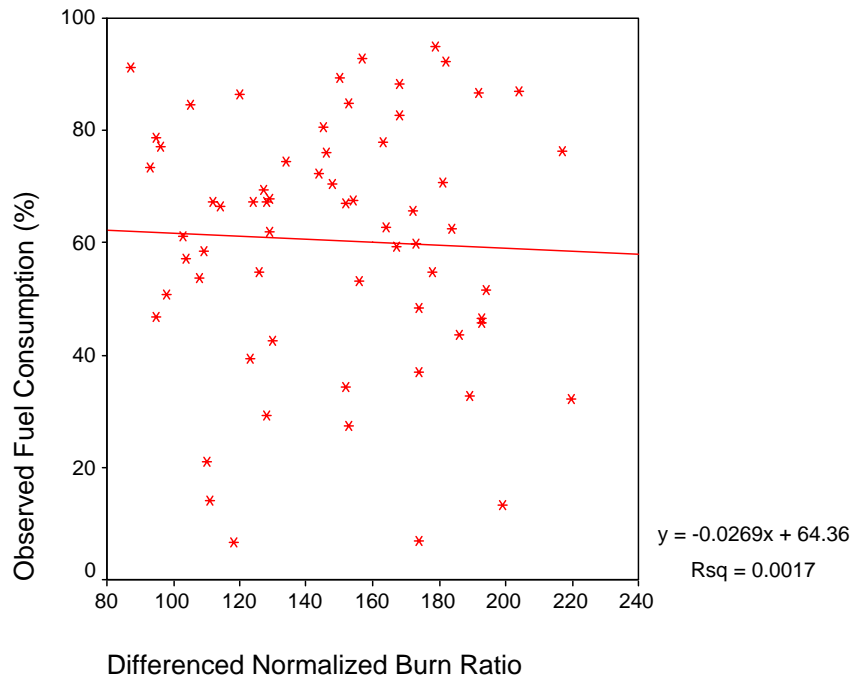


Figure 5. Relationship between observed tree mortality (%) and FIREHARM tree mortality (%). The dashed red line is a 1:1 line, while the solid black line is the regression trend line.

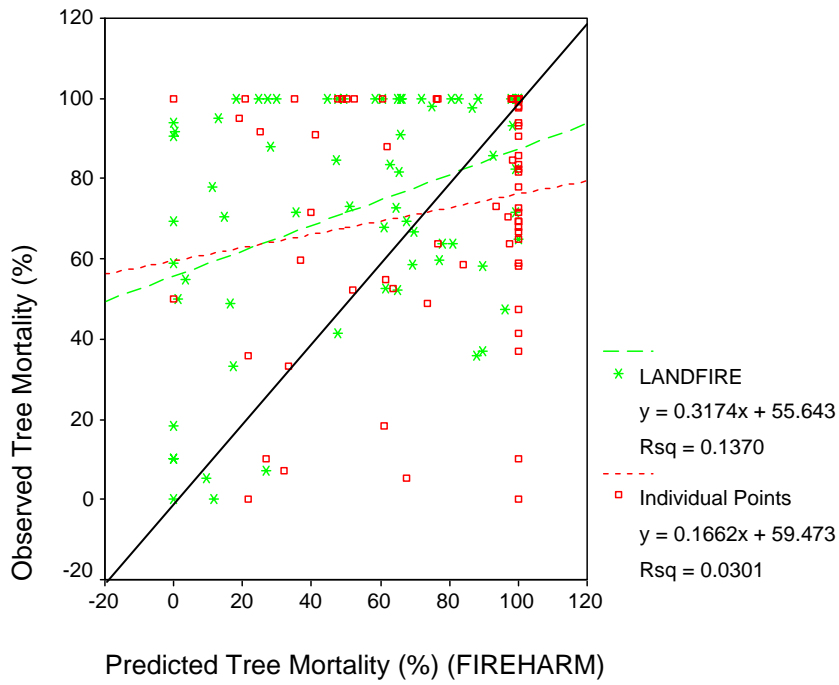


Figure 6. Association between observed tree mortality (%) and the Differenced Normalized Burn Ratio. The solid black line is the regression trend line.

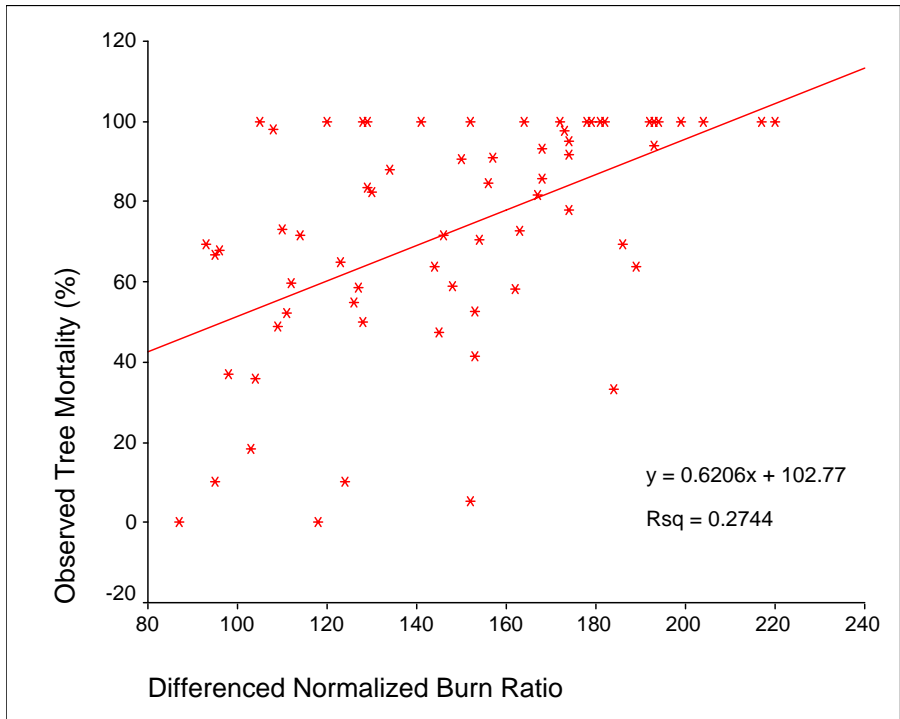


Figure 7. Maps of burn severity and fire effects for the Cooney Ridge fire. A. Differenced Normalized Burn Ratio (scaled from 0-255). B. FIREHARM simulated Fuel Consumption (%) C. FIREHARM simulated Tree Mortality (%).

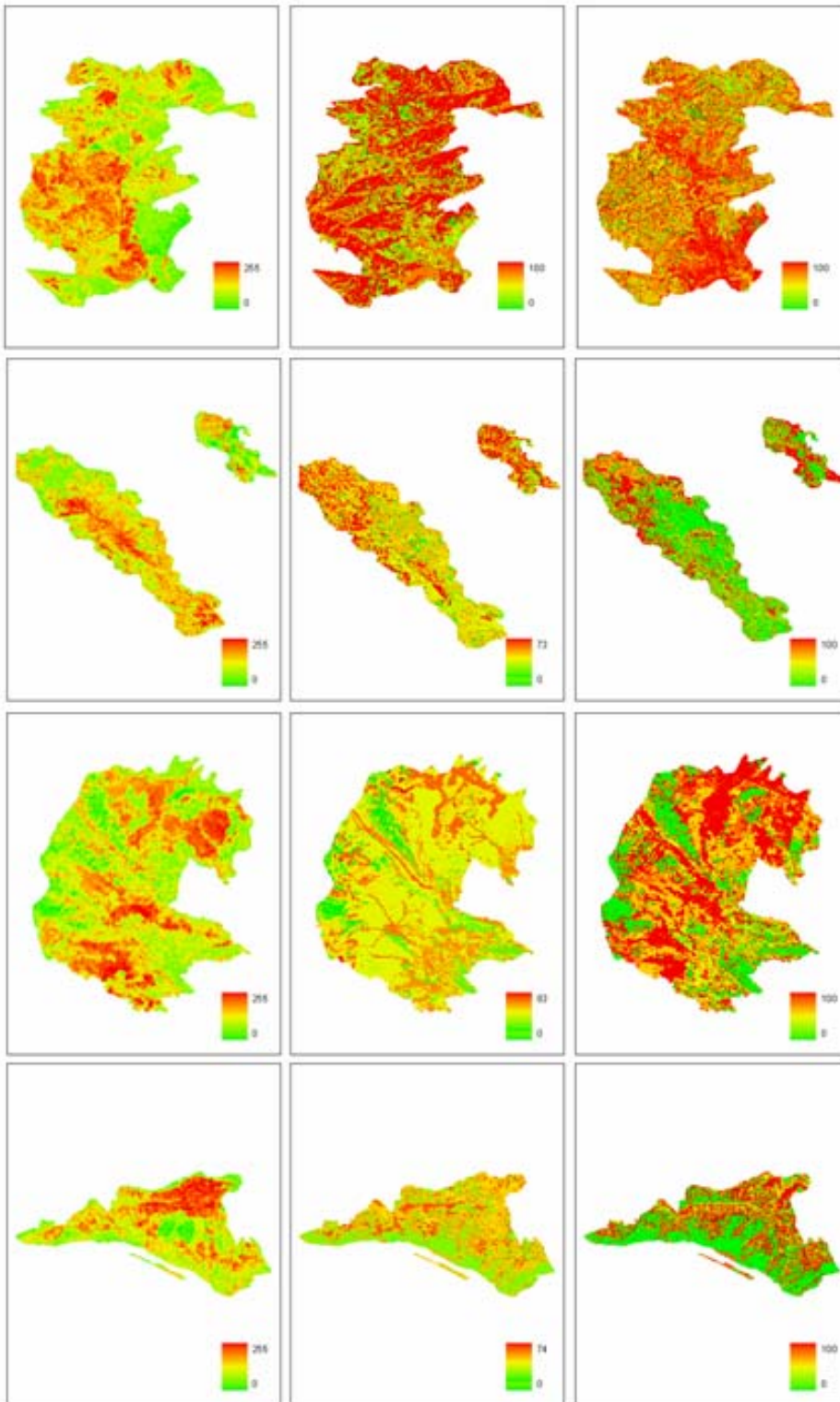


Figure 8. Satellite and Model-derived maps of burn severity for the four fire areas (arranged in rows from first to last: Cooney Ridge, Mineral Primm, Gash Creek and I90 Complex). Column 1: Δ NBR (classed as Low, Moderate and High Burn Severity). Column 2: FIREHARM Burn Severity (classed as Low, Moderate and High Burn Severity) Column 3: difference map showing discrepancy and agreement between Δ NBR and FIREHARM burn severity maps (red means Δ NBR severity was lower than FIREHARM severity, blue means the maps are in agreement, and yellow means Δ NBR severity was higher than FIREHARM severity).

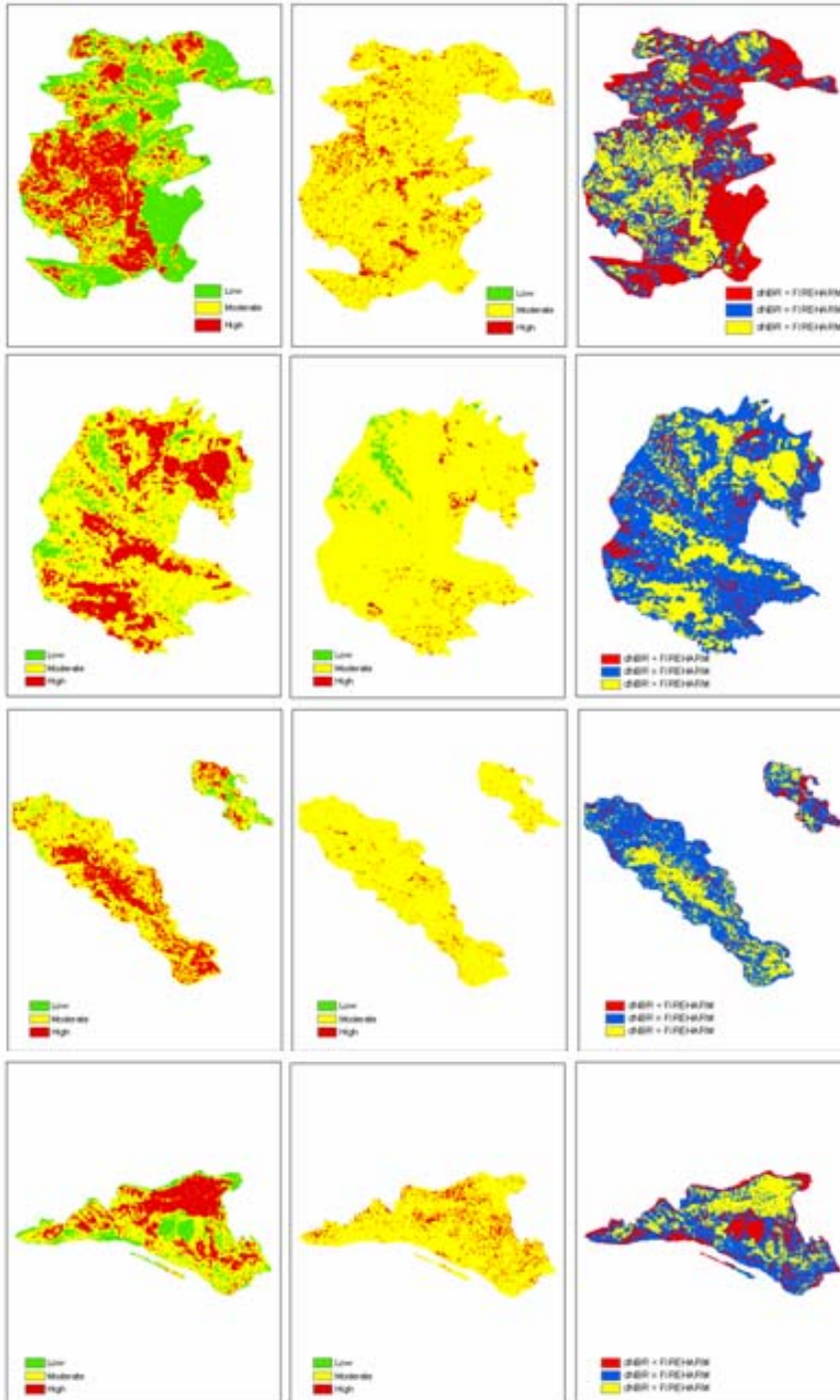


Figure 9. Relationship between FIREHARM modeled fuel consumption and tree mortality (LANDFIRE parameterization) for the Cooney Ridge fire. Points are labeled by equal interval Δ NBR classes of the continuous Δ NBR image (red, yellow and green symbols represent Δ NBR = 3, 2 and 1, respectively).

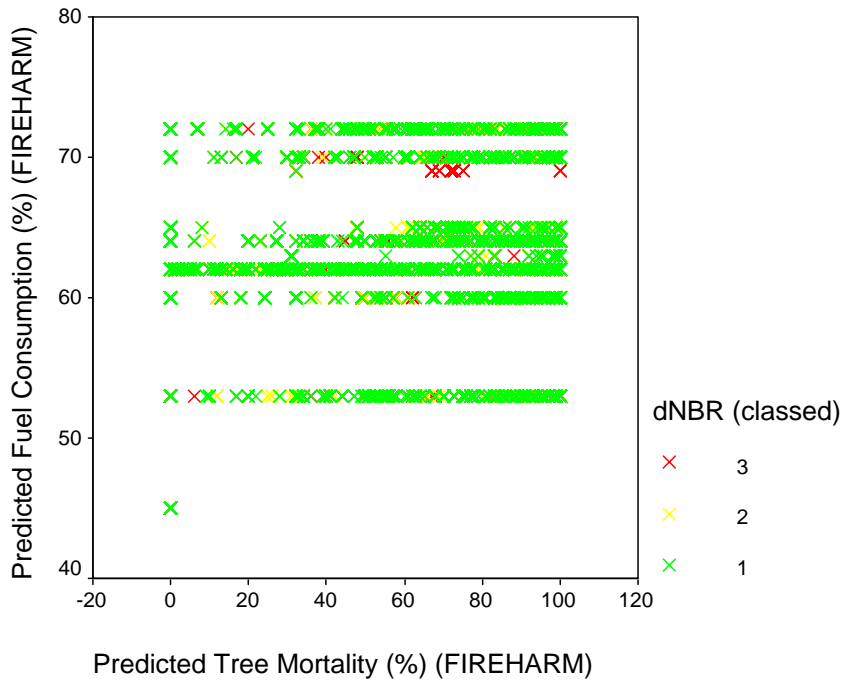


Figure 10. Relationship between FIREHARM modeled fuel consumption and tree mortality for a) LANDFIRE-based and b) Individual Plot-based parameterizations. Points are labeled by Composite Burn Index, rounded to the nearest integer (red circles, yellow squares and green stars represent CBI = 3, 2 and 1, respectively).

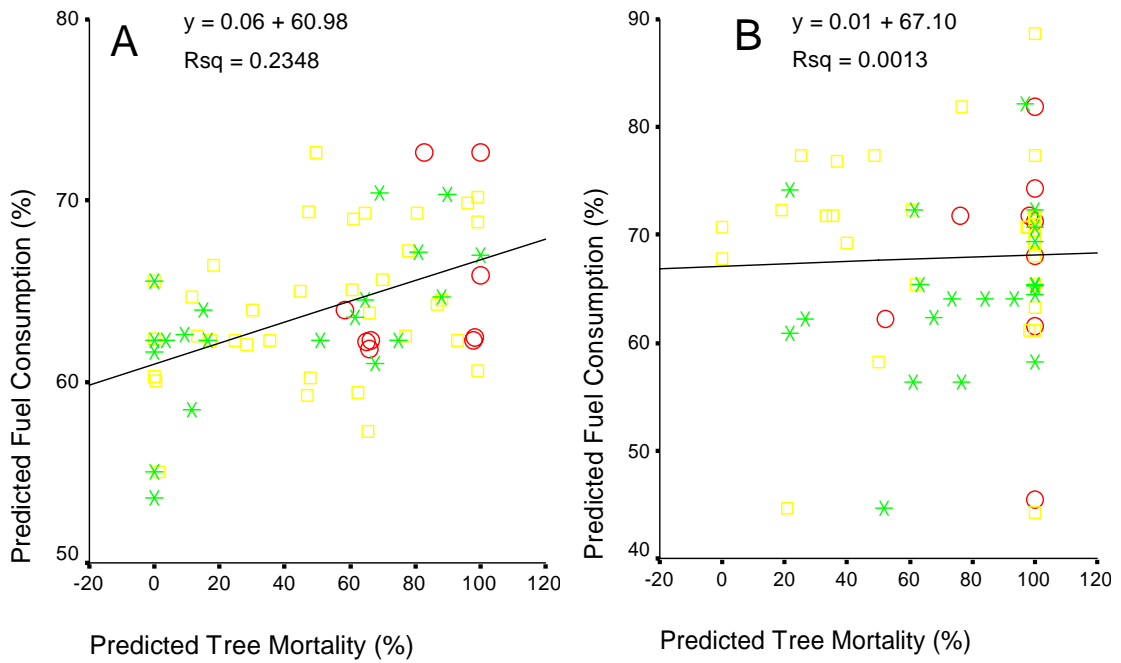


Figure 11. Relationship between Differenced Normalized Burn Ratio (continuous) and FIREHARM modeled fuel consumption (a,b), and tree mortality (c,d) for both LANDFIRE (a,c) and Individual Plot (b,d) parameterizations. Points are labeled by Composite Burn Index, rounded to the nearest integer (red circles, yellow squares and green stars represent CBI = 3, 2 and 1, respectively).

